

Fermionic current from topology and boundaries with applications to nanotubes

S. Bellucci^{1*} and A. A. Saharian^{2†}

¹ *INFN, Laboratori Nazionali di Frascati,
Via Enrico Fermi 40, 00044 Frascati, Italy*

² *Department of Physics, Yerevan State University,
1 Alex Manoogian Street, 0025 Yerevan, Armenia*

July 24, 2012

Abstract

We investigate combined effects of topology and boundaries on the vacuum expectation value (VEV) of the fermionic current in the space with an arbitrary number of toroidally compactified dimensions. As a geometry of boundaries we consider two parallel plates on which the fermion field obeys bag boundary conditions. Along the compact dimensions, periodicity conditions are imposed with arbitrary phases. In addition, the presence of a constant gauge field is assumed. The nontrivial topology gives rise to an Aharonov-Bohm effect for the fermionic current induced by the gauge field. It is shown that the VEV of the charge density vanishes and the current density has nonzero expectation values for the components along compact dimensions only. The latter are periodic odd functions of the magnetic flux with the period equal to the flux quantum. In the region between the plates, the VEV of the fermionic current is decomposed into pure topological, single plate and interference parts. For a massless field the single plate part vanishes and the interference part is distributed uniformly. The corresponding results are generalized for conformally-flat spacetimes. Applications of the general formulas to finite-length carbon nanotubes are given within the framework of the Dirac model for quasiparticles in graphene. In the absence of the magnetic flux, two sublattices of the honeycomb graphene lattice yield opposite contributions and the fermionic current vanishes. A magnetic flux through the cross section of the nanotube breaks the symmetry allowing the current to flow along the compact dimension.

PACS numbers: 03.70.+k, 11.10.Kk, 61.46.Fg

1 Introduction

In quantum field theory, the boundary conditions imposed on the field operator give rise to a number of interesting physical effects. In the first class of models, these conditions are due to presence of boundaries having different physical nature, like macroscopic bodies in QED, extended topological defects, horizons and so on. In this type of problems the field operator obeys the boundary condition on some space-like surfaces. A well-known quantum effect induced

*E-mail: bellucci@lnf.infn.it

†E-mail: saharian@ysu.am

by this kind of boundary conditions is the Casimir effect (for reviews see Ref. [1]). The Casimir effect is among the most striking macroscopic manifestations of nontrivial properties of the quantum vacuum. The boundary conditions imposed on the field operator alter the zero-point modes of a quantized field and shift the vacuum expectation values (VEVs) of quantities, such as the energy density and stresses. This leads to the appearance of forces acting on constraining boundaries.

In the second class of models, the boundary conditions arise due to the nontrivial topology of the space. The latter induces periodicity conditions imposed on the field operator along compact dimensions. This type of models appear in many high-energy theories of fundamental physics, including supergravity and superstring theories. Models of a compact universe with nontrivial topology may also play an important role by providing proper initial conditions for inflation in the early stages of the Universe expansion [2]. An interesting application of the field theoretical models with compact dimensions appeared in nanophysics recently. For long-wavelengths, the dynamics of quasiparticles in a graphene sheet is well described in terms of the Dirac-like theory in 2-dimensional space with the Fermi velocity playing the role of the speed of light (see Ref. [3]). In the geometry of a single-walled carbon nanotube, which is generated by rolling up a graphene sheet to form a cylinder, the background space for the corresponding Dirac model has topology $R^1 \times S^1$. For toroidal carbon nanotubes, an additional compactification along the tube axis leads to the topology $(S^1)^2$.

In models with nontrivial topology, the periodicity conditions along compact dimensions give rise to Casimir-type contributions in the VEVs of various physical observables. In Kaluza-Klein models, the topological Casimir effect has been used for the stabilization of moduli fields and as a source for dynamical compactification of extra dimensions. As it has been discussed in Refs. [4], the Casimir energy related to the compact subspace of extra dimensions can serve as a model for dark energy driving the accelerated expansion of the universe at the present epoch. Note that, the recent measurements of the Casimir forces between macroscopic bodies provide a sensitive test to constrain the parameters of various types of long-range interactions predicted by unification theories [5]. The influence of extra compactified dimensions on the Casimir effect in the geometry of two parallel plates has been recently discussed for scalar [6], electromagnetic [7], and Dirac fermion [8, 9] fields. The combined quantum vacuum effects from boundaries (branes) and from the non-trivial topology of spatial dimensions in braneworld models on anti-de Sitter bulk are considered in Ref. [10] (for the Casimir energy and stresses in braneworlds see Ref. [11]). In these models the Casimir forces provide a natural mechanism for stabilizing the radion field, as required for a complete solution of the hierarchy problem between the gravitational and electroweak mass scales.

In the papers cited above, the vacuum energy and the forces acting on the constraining boundaries were considered. For charged fields an additional important characteristic of the vacuum state, bilinear in the field, is the VEV of the current density. In Ref. [12], the VEV of the current density is evaluated for a massive fermionic field in spaces with toroidally compactified dimensions. It has been shown that the nontrivial topology of the background spacetime leads to the Aharonov-Bohm effect for the fermionic current induced by the gauge field. Continuing in this line of investigation, in the present paper we consider the combined effects of boundaries and compact spatial dimensions on the VEV of the fermionic current. Although the corresponding operator is local, due to the global nature of the vacuum, this quantity carries an important information about the topology of the background space. The current acts as the source in the Maxwell equations and therefore plays an important role in modelling a self-consistent dynamics involving the electromagnetic field. As the boundary geometry here we will consider two parallel plates on which the fermionic field obeys the MIT bag boundary condition. In addition, we assume the presence of a constant gauge field (the fermionic current in a conical space with a

circular boundary has been recently discussed in Ref. [13]).

The outline of the paper is as follows. In the next section, we specify the mode functions and the eigenvalues of the momentum for the Dirac equation in the region between two plates with bag boundary conditions on them. The VEV of the fermionic current in this region is investigated in Sect. 3. This VEV is decomposed into a pure topological, single plate and interference parts. We also give a generalization for conformally-flat background spacetimes with toroidally compact dimensions. In Sect. 4 we apply the general formulas for the investigation of the fermionic current in finite-length metallic and semiconductor carbon nanotubes, within the framework of the Dirac model for quasiparticles in graphene. The main results of the paper are summarized in Sect. 5. In Appendix we derive an alternative expression for the VEV of the fermionic current in the geometry of a single plate.

2 Mode functions

We consider a Dirac fermion field $\psi(x)$ in background of a $(D + 1)$ -dimensional flat spacetime, in the presence of a gauge field A_μ . The dynamics of the field is described by the Dirac equation

$$(i\gamma^\mu D_\mu - m)\psi(x) = 0, \quad (1)$$

with $D_\mu = \partial_\mu + ieA_\mu$. The dimensions for Dirac matrices $\gamma^\mu = (\gamma^0, \boldsymbol{\gamma})$ are $N_D \times N_D$, where $N_D = 2^{[(D+1)/2]}$ and the square brackets denote the integer part of $(D + 1)/2$. In the discussion below we use the Dirac representation:

$$\gamma^0 = \begin{pmatrix} 1 & 0 \\ 0 & -1 \end{pmatrix}, \quad \boldsymbol{\gamma} = \begin{pmatrix} 0 & \boldsymbol{\sigma} \\ -\boldsymbol{\sigma}^+ & 0 \end{pmatrix}, \quad (2)$$

with $\boldsymbol{\sigma} = (\sigma_1, \dots, \sigma_D)$. For the matrices σ_μ in Eq. (2) we have the anticommutation relations $\sigma_\mu \sigma_\nu^+ + \sigma_\nu \sigma_\mu^+ = 2\delta_{\mu\nu}$. In a two-dimensional space the irreducible representation corresponds to $N_D = 2$ and the corresponding Dirac matrices can be taken as $\gamma^\mu = (\sigma_{P3}, i\sigma_{P1}, i\sigma_{P2})$, where $\sigma_{P\mu}$ are the Pauli matrices.

We assume that $q = D - p - 1$ spatial dimensions with the Cartesian coordinates $\mathbf{z}_q = (z_{p+2}, \dots, z_D)$ are toroidally compactified. The length of the l -th compact dimension will be denoted by L_l , so $0 \leq z_l \leq L_l$ for $l = p + 2, \dots, D$. The remaining coordinates $\mathbf{z}_{p+1} = (z_1, \dots, z_{p+1} \equiv z)$ are not compactified with $-\infty < z_l < \infty$, $l = 1, \dots, p + 1$. Hence, we consider the background space with topology $R^{p+1} \times (S^1)^q$. Along the compact dimensions we impose on the field operator quasiperiodic boundary conditions:

$$\psi(t, \mathbf{z}_{p+1}, \mathbf{z}_q + L_l \mathbf{e}_l) = e^{2\pi i \alpha_l} \psi(t, \mathbf{z}_{p+1}, \mathbf{z}_q), \quad (3)$$

with constant phases $|\alpha_l| \leq 1/2$ and with \mathbf{e}_l being the unit vector along the direction of the coordinate z_l , $l = p + 2, \dots, D$. For untwisted and twisted fermionic fields one has special values $\alpha_l = 0$ and $\alpha_l = 1/2$, respectively.

Our main interest in this paper is the VEV of the fermionic current $j^\mu = \bar{\psi} \gamma^\mu \psi$, where $\bar{\psi} = \psi^\dagger \gamma^0$ is the Dirac adjoint and, as usual, the dagger denotes Hermitian conjugation. We assume the presence of two parallel plates placed at $z = 0$ and $z = a$, on which the field operator obeys MIT bag boundary conditions

$$(1 + i\gamma^\mu n_\mu) \psi(x) = 0, \quad z = 0, a, \quad (4)$$

where n_μ is the outward oriented normal to the boundary. From these conditions it follows that on the boundaries $n_\mu j^\mu = 0$, i.e. the component of the current along the normal to the

boundaries vanishes on the plates. In what follows we will consider the region between the plates, $0 < z < a$, with $n_\mu = -\delta_\mu^{p+1}$ and $n_\mu = \delta_\mu^{p+1}$ for the plates at $z = 0$ and $z = a$, respectively. The expressions for the VEVs in the regions $z < 0$ and $z > a$ are obtained by the limiting transition.

The VEV of the fermionic current is expressed in terms of the two-point function $S_{rs}^{(1)}(x, x') = \langle 0 | [\psi_r(x), \bar{\psi}_s(x')] | 0 \rangle$, where r, s are spinor indices and $|0\rangle$ stands for the vacuum state. The expression for the VEV reads:

$$\langle j^\mu(x) \rangle \equiv \langle 0 | j^\mu(x) | 0 \rangle = -\frac{1}{2} \text{Tr}(\gamma^\mu S^{(1)}(x, x)). \quad (5)$$

Let $\{\psi_\beta^{(+)}(x), \psi_\beta^{(-)}(x)\}$ be a complete set of positive- and negative-energy solutions to the Dirac equation with a set of quantum numbers β specifying the modes (see below). Expanding the fermionic field operator in terms of these solutions with the coefficients being the annihilation and creation operators, the VEV of the current is presented in the form of the mode sum

$$\langle j^\mu \rangle = \frac{1}{2} \sum_\beta [\bar{\psi}_\beta^{(-)}(x) \gamma^\mu \psi_\beta^{(-)}(x) - \bar{\psi}_\beta^{(+)}(x) \gamma^\mu \psi_\beta^{(+)}(x)]. \quad (6)$$

This expression is divergent, hence some regularization and subsequent renormalization procedure is necessary. The important point here is that, owing to the flatness of the background spacetime, the structure of divergences is the same as for the topologically trivial Minkowski spacetime. As a result, the renormalization is reduced to the subtraction from the VEV of the corresponding Minkowskian quantity. In what follows, in order to make the expression on the right-hand side of Eq. (6) finite, we will assume the presence of some cutoff function, without writing it explicitly. The special form of the latter will not be important in the remainder of the discussion.

For the evaluation of the VEV by Eq. (6) we need to have the mode functions $\psi_\beta^{(\pm)}(x)$ for the equation (1) obeying the periodicity conditions (3) and the boundary conditions (4). For the gauge field we assume that $A_\mu = \text{const}$. Although the corresponding field strength vanishes, the nontrivial topology of the space leads to the Aharonov-Bohm-like effect for the fermionic current. In the problem under consideration, the mode sum (6) involves the integration over the momentum along uncompactified dimensions and the components of the constant gauge field along these dimensions are simply removed by shifting the integration variable. Consequently, the VEV does not depend on these components. For that reason we will assume a nonzero vector potential along compact dimensions only: $A_\mu = (0, -\mathbf{A})$ with $\mathbf{A} = (0, \mathbf{A}_q)$ and $\mathbf{A}_q = (A_{p+2}, \dots, A_D)$.

With this choice, the mode functions are obtained from those discussed in Ref. [9] by a simple generalization:

$$\begin{aligned} \psi_\beta^{(+)} &= A_\beta^{(+)} e^{-i\omega^{(+)}t} \left(\frac{-i}{\omega^{(+)}+m} \boldsymbol{\sigma}^+ \cdot (\boldsymbol{\nabla} - ie\mathbf{A}) \varphi^{(+)} \right), \\ \psi_\beta^{(-)} &= A_\beta^{(-)} e^{i\omega^{(-)}t} \left(\frac{i}{\omega^{(-)}+m} \boldsymbol{\sigma}^- \cdot (\boldsymbol{\nabla} - ie\mathbf{A}) \varphi^{(-)} \right), \end{aligned} \quad (7)$$

For the upper and lower components of the positive- and negative-energy functions one has the expressions

$$\varphi^{(\pm)} = e^{\pm i\mathbf{k}_\parallel^{(\pm)} \cdot \mathbf{z}_\parallel} (\varphi_+^{(\pm)} e^{ik_{p+1}z} + \varphi_-^{(\pm)} e^{-ik_{p+1}z}), \quad (8)$$

with $\mathbf{z}_\parallel = (z_1, \dots, z_p, z_{p+2}, \dots, z_D)$ being the coordinates parallel to the plates. For the corresponding momentum we have $\mathbf{k}_\parallel^{(\pm)} = (\mathbf{k}_p, \mathbf{k}_q^{(\pm)})$ and $\mathbf{k}_p = (k_1, \dots, k_p)$, $\mathbf{k}_q^{(\pm)} = (k_{p+2}, \dots, k_D^{(\pm)})$.

Now, the energy corresponding to the modes reads

$$\omega^{(\pm)} = \sqrt{\mathbf{k}_p^2 + k_{p+1}^2 + (\mathbf{k}_q^{(\pm)} \mp e\mathbf{A}_q)^2 + m^2}. \quad (9)$$

From the periodicity conditions (3), for the eigenvalues of the momentum components along the compact dimensions we find

$$k_l^{(\pm)} = 2\pi(n_l \pm \alpha_l)/L_l, \quad l = p+2, \dots, D, \quad (10)$$

with $n_l = 0, \pm 1, \pm 2, \dots$. For the components along the uncompactified dimensions one has $-\infty < k_l < \infty$, $l = 1, \dots, p$.

The relations between the coefficients in Eq. (8) is found from the boundary condition (4) on the plate at $z = 0$:

$$\begin{aligned} \varphi_+^{(+)} &= \frac{k_{p+1}\sigma_{p+1}\boldsymbol{\sigma}_{\parallel}^+ \cdot (\mathbf{k}_{\parallel}^{(+)} - e\mathbf{A}) - m(\omega^{(+)} + m) - k_{p+1}^2}{(m - ik_{p+1})(\omega^{(+)} + m)}\varphi_-^{(+)}, \\ \varphi_-^{(-)} &= \frac{k_{p+1}\sigma_{p+1}\boldsymbol{\sigma}_{\parallel}^+ \cdot (\mathbf{k}_{\parallel}^{(-)} + e\mathbf{A}) - m(\omega^{(-)} + m) - k_{p+1}^2}{(m + ik_{p+1})(\omega^{(-)} + m)}\varphi_+^{(-)}, \end{aligned} \quad (11)$$

where $\boldsymbol{\sigma}_{\parallel} = (\sigma_1, \dots, \sigma_p, \sigma_{p+2}, \dots, \sigma_D)$. As we have already extracted the coefficients $A_{\beta}^{(\pm)}$ in Eq. (7), we can impose the normalization conditions $\varphi_-^{(+)+}\varphi_-^{(+)} = \varphi_+^{(-)+}\varphi_+^{(-)} = 1$. Now, from Eq. (11) it can be seen that one has also the relations $\varphi_+^{(+)+}\varphi_+^{(+)} = \varphi_-^{(-)+}\varphi_-^{(-)} = 1$. As a set of independent spinors with this normalization we take $\varphi_-^{(+)} = w^{(\sigma)}$ and $\varphi_+^{(-)} = w^{(\sigma)'}.$ Here $w^{(\sigma)}$, $\sigma = 1, \dots, N_D/2$, are one-column matrices having $N_D/2$ rows with the elements $w_l^{(\sigma)} = \delta_{l\sigma}$, and $w^{(\sigma)'} = iw^{(\sigma)}$.

It remains for us to impose on the mode functions the boundary condition (4) on the plate at $z = a$. From this condition we find the following equation for the eigenvalues of the component of the momentum normal to the plates:

$$ma \sin(k_{p+1}a)/(k_{p+1}a) + \cos(k_{p+1}a) = 0. \quad (12)$$

We denote the positive solutions of this equation, arranged in the ascending order, by $\lambda_n = k_{p+1}a$, $n = 1, 2, \dots$. Note that, for a massless field, one has $\lambda_n = \pi(n - 1/2)$. Hence, the mode functions (7) are specified by the set $\beta = (\mathbf{k}_p, \mathbf{k}_q^{(\pm)}, n, \sigma)$.

The coefficients $A_{\beta}^{(\pm)}$ in Eq. (7) are determined from the normalization condition with the integration over the region between the plates. They are given by the expression

$$A_{\beta}^{(\pm)2} = \frac{\omega^{(\pm)} + m}{4(2\pi)^p \omega^{(\pm)} a V_q} \left[1 - \frac{\sin(2\lambda_n)}{2\lambda_n} \right]^{-1}, \quad (13)$$

with $V_q = L_{p+2} \cdots L_D$ being the volume of the compact subspace.

3 Fermionic current

Having the complete set of mode functions, we can evaluate the VEV of the fermionic current by using the mode sum formula (6). First of all, we consider the $\mu = 0$ component which corresponds to the vacuum charge density.

3.1 Charge density

By taking into account Eq. (7) for the positive- and negative-energy mode functions, for the charge density one finds the expression below:

$$\begin{aligned} \langle j^0 \rangle &= \frac{N_D}{4aV_q} \sum_{\mathbf{n}_q \in \mathbf{Z}^q} \int \frac{d\mathbf{k}_p}{(2\pi)^p} \sum_{n=1}^{\infty} \left[1 - \frac{\sin(2\lambda_n)}{2\lambda_n} \right]^{-1} \\ &\times \left[2 - ma \left(\frac{e^{2i\lambda_n z/a}}{ma - i\lambda_n} + \frac{e^{-2i\lambda_n z/a}}{ma + i\lambda_n} \right) \right]. \end{aligned} \quad (14)$$

where $\mathbf{n}_q = (n_{p+2}, \dots, n_D)$, $-\infty < n_l < +\infty$. This expression is not convenient for the direct evaluation of the charge density. This is related to the fact that the eigenvalues λ_n are given implicitly and the terms with large values of n are highly oscillatory. These two problems are solved by using the Abel-Plana-type summation formula [14, 15]

$$\sum_{n=1}^{\infty} \frac{\pi f(\lambda_n)}{1 - \sin(2\lambda_n)/(2\lambda_n)} = -\frac{\pi m a f(0)}{2(ma + 1)} + \int_0^{\infty} dx f(x) - i \int_0^{\infty} dx \frac{f(ix) - f(-ix)}{\frac{x+ma}{x-ma} e^{2x} + 1}. \quad (15)$$

The corresponding function $f(x)$ in Eq. (14) is an even function and, hence, the last integral in Eq. (15) vanishes. In addition, one has $f(0) = 0$. Further, for the part in the first integral in the right-hand side of Eq. (15) we have

$$\int_0^{\infty} dx \left(\frac{e^{-2ixz_{p+1}}}{m + ix} + \frac{e^{2ixz_{p+1}}}{m - ix} \right) = 0. \quad (16)$$

Hence, after applying Eq. (15) we get:

$$\langle j^0 \rangle = \frac{N_D}{2aV_q} \int \frac{d\mathbf{k}_{p+1}}{(2\pi)^{p+1}} \sum_{\mathbf{n}_q \in \mathbf{Z}^q} 1. \quad (17)$$

The latter coincides with the charge density in the spacetime with topology $R^{p+1} \times (S^1)^q$, in the absence of boundaries. The renormalized value of the latter vanishes [12]. Hence, we conclude that the presence of boundaries with MIT bag boundary conditions does not induce any vacuum charge density.

3.2 Current density

Next we consider the spatial components for $\langle j^\mu \rangle$, $\mu = 1, \dots, D$. Firstly, let us consider the component of the current along the direction normal to the plates. From Eqs. (6) and (7) the following expression is obtained

$$\langle j^{p+1} \rangle = \frac{i}{2} \sum_{j=+,-} \sum_{\beta} \frac{A_{\beta}^{(j)2}}{\omega^{(j)} + m} [\varphi^{(j)+} \partial_{p+1} \varphi^{(j)} - (\partial_{p+1} \varphi^{(j)+}) \varphi^{(j)}]. \quad (18)$$

By making use of Eq. (8), it can be seen that

$$\varphi^{(j)+} \partial_{p+1} \varphi^{(j)} - (\partial_{p+1} \varphi^{(j)+}) \varphi^{(j)} = 2ik_{p+1} (\varphi_+^{(j)+} \varphi_+^{(j)} - \varphi_-^{(j)+} \varphi_-^{(j)}) = 0. \quad (19)$$

Hence, we conclude that the VEV of the normal component of the fermionic current vanishes.

Now we turn to the components of the current along the directions parallel to the plates. From Eqs. (6) and (7) we get

$$\langle j^l \rangle = \sum_{j=+,-} \sum_{\beta} \frac{A_{\beta}^{(j)2}}{\omega^{(j)} + m} [-jk_l^{(j)} \varphi^{(j)+} \varphi^{(j)} + \frac{i}{2} \partial_{p+1} (\varphi^{(j)+} \sigma_l^{(j')} \sigma_{p+1}^{(j)} \varphi^{(j)})],$$

where $l = 1, \dots, p, p+2, \dots, D$, $j' = +$ for $j = -$ and $j' = -$ for $j = +$. We have also used the notations $\sigma_{\mu}^{(-)} = \sigma_{\mu}$ and $\sigma_{\mu}^{(+)} = \sigma_{\mu}^+$. By using Eqs. (8) and (11), after lengthy calculations, the following representation is obtained for the corresponding mode sum in the region between the plates:

$$\begin{aligned} \langle j^l \rangle &= \frac{N_D}{4aV_q} \sum_{\mathbf{n}_q \in \mathbf{Z}^q} \int \frac{d\mathbf{k}_p}{(2\pi)^p} \sum_{n=1}^{\infty} \left[1 - \frac{\sin(2\lambda_n)}{2\lambda_n} \right]^{-1} \\ &\times \frac{k_l}{\omega} \left[2 - ma \left(\frac{e^{2i\lambda_n z/a}}{ma - i\lambda_n} + \frac{e^{-2i\lambda_n z/a}}{ma + i\lambda_n} \right) \right], \end{aligned} \quad (20)$$

where

$$k_l = 2\pi(n_l + \tilde{\alpha}_l)/L_l \text{ for } l = p+2, \dots, D, \quad (21)$$

and

$$\omega = \sqrt{\lambda_n^2/a^2 + \mathbf{k}_p^2 + \mathbf{k}_q^2 + m^2}, \quad (22)$$

with $\mathbf{k}_q = (k_{p+2}, \dots, k_D)$. In Eq. (21) we have defined

$$\tilde{\alpha}_l = eA_l L_l / (2\pi) - \alpha_l. \quad (23)$$

Hence, the VEV of the fermionic current depends on the phases in the periodicity conditions and on the components of the vector potential in the combination (23). From Eq. (20) it follows that the VEV is a periodic odd function of this parameter with the period equal to 1. In particular, the fermionic current is a periodic function of $A_l L_l$ with the period of the flux quantum $\Phi_0 = 2\pi/|e|$ ($\Phi_0 = 2\pi\hbar c/|e|$ in standard units).

From Eq. (20) it directly follows that the components of the current density along the uncompactified dimensions vanish:

$$\langle j^l \rangle = 0 \text{ for } l = 1, \dots, p. \quad (24)$$

We also can see that the fermionic current along the l -th compact dimension vanishes for the special cases $\tilde{\alpha}_l = 0$ and $\tilde{\alpha}_l = 1/2$. In particular, this is the case for untwisted and twisted fermion fields in the absence of the gauge field.

By the reasons given after Eq. (14), formula (20) is not convenient for the investigation of the properties of the current. In order to obtain a more workable representation, for the summation of the series over n we use Eq. (15). As a result, the VEV of the current is decomposed as:

$$\begin{aligned} \langle j^l \rangle &= \langle j^l \rangle^{(0)} + \langle j^l \rangle^{(1)} - \frac{N_D}{2\pi V_q} \sum_{\mathbf{n}_q \in \mathbf{Z}^q} k_l \int \frac{d\mathbf{k}_p}{(2\pi)^p} \int_{\sqrt{k_{\parallel}^2 + m^2}}^{\infty} dx \\ &\times \frac{(x^2 - k_{\parallel}^2 - m^2)^{-1/2}}{\frac{x+m}{x-m} e^{2ax} + 1} \left[2 - m \left(\frac{e^{2zx}}{m-x} + \frac{e^{-2zx}}{m+x} \right) \right] \Bigg\}, \end{aligned} \quad (25)$$

where $k_{\parallel}^2 = \mathbf{k}_p^2 + \mathbf{k}_q^2$. Note that the first two terms in the right-hand side of Eq. (25) come from the first integral in the right-hand side of Eq. (15). In Eq. (25),

$$\langle j^l \rangle^{(0)} = \frac{N_D}{2V_q} \sum_{\mathbf{n}_q \in \mathbf{Z}^q} \int \frac{d\mathbf{k}_{p+1}}{(2\pi)^{p+1}} \frac{k_l}{\sqrt{\mathbf{k}_{p+1}^2 + \mathbf{k}_q^2 + m^2}}, \quad (26)$$

is the corresponding fermionic current in the boundary-free spacetime with topology $R^{p+1} \times (S^1)^q$ and the part

$$\begin{aligned} \langle j^l \rangle^{(1)} &= -\frac{N_D m}{4\pi V_q} \int \frac{d\mathbf{k}_p}{(2\pi)^p} \sum_{\mathbf{n}_q \in \mathbf{Z}^q} k_l \int_0^\infty dx \\ &\quad \times \frac{e^{2ixz}/(m-ix) + e^{-2ixz}/(m+ix)}{\sqrt{x^2 + \mathbf{k}_p^2 + \mathbf{k}_q^2 + m^2}}, \end{aligned} \quad (27)$$

is induced by the presence of a single plate located at $z = 0$, when the second plate is absent. The latter can be seen by the direct evaluation of the VEV for a single plate, or by taking the limit $a \rightarrow \infty$ in Eq. (25). Hence, the last term in Eq. (25) can be interpreted as being induced by the presence of the second plate at $z = a$.

The boundary induced parts in Eq. (25) are finite (see below) and the renormalization is necessary for the boundary-free part only. The latter has been investigated in Ref. [12]. The corresponding renormalized VEV is given by the expression

$$\begin{aligned} \langle j^l \rangle^{(0)} &= \frac{2N_D m^{D+1} L_l}{(2\pi)^{(D+1)/2}} \sum_{n_l=1}^{\infty} n_l \sin(2\pi n_l \tilde{\alpha}_l) \\ &\quad \times \sum_{\mathbf{n}_{q-1} \in \mathbf{Z}^{q-1}} \cos(2\pi \mathbf{n}_{q-1} \cdot \boldsymbol{\alpha}_{q-1}) \frac{K_{(D+1)/2}(mg(\mathbf{L}_q, \mathbf{n}_q))}{(mg(\mathbf{L}_q, \mathbf{n}_q))^{(D+1)/2}}, \end{aligned} \quad (28)$$

where $\mathbf{n}_{q-1} = (n_{p+2}, \dots, n_{l-1}, n_{l+1}, \dots, n_D)$, $\boldsymbol{\alpha}_{q-1} = (\tilde{\alpha}_{p+1}, \dots, \tilde{\alpha}_{l-1}, \tilde{\alpha}_{l+1}, \dots, \tilde{\alpha}_D)$, $K_\nu(x)$ is the Macdonald function (i.e. the modified Bessel function of the second kind) and

$$g(\mathbf{L}_q, \mathbf{n}_q) = \left(\sum_{i=p+2}^D L_i^2 n_i^2 \right)^{1/2}. \quad (29)$$

The reason for the sign difference of α_l in the expression of $\tilde{\alpha}_l$ in Eq. (23) and in the corresponding expression of Ref. [12] is that, in the latter reference, for the evaluation of the VEV the negative-energy modes have been used, with the eigenvalues $k_l^{(+)}$ (see Eq. (10)) instead of $k_l^{(-)}$. This means that, in fact, the formulas given in Ref. [12] are for the periodicity conditions (3) with α_l replaced by $-\alpha_l$. The formula (28) is obtained by making use of the zeta function technique. An alternative representation, derived by using the Abel-Plana-type summation formula, is given in Rev. [12]. In the discussion below we will be mainly concerned with the effects induced by the plates.

3.2.1 Fermionic current induced by a single plate

First of all, we discuss the part in the fermionic current induced by a single plate. As it is seen from Eq. (27), for a massless field the latter vanishes. In the case of a massive field, for the further transformation of Eq. (27), we rotate the integration contour in the complex plane x by

the angle $\pi/2$ for the term with e^{2ixz} and by the angle $-\pi/2$ for the term with e^{2ixz} . This gives the result:

$$\langle j^l \rangle^{(1)} = -\frac{N_D m}{(2\pi)^{p+1} V_q} \sum_{\mathbf{n}_q \in \mathbf{Z}^q} k_l \int d\mathbf{k}_p \int_{\sqrt{\mathbf{k}_p^2 + m_{\mathbf{n}_q}^2}}^{\infty} dx \frac{e^{-2xz/(m+x)}}{\sqrt{x^2 - \mathbf{k}_p^2 - m_{\mathbf{n}_q}^2}}, \quad (30)$$

where

$$m_{\mathbf{n}_q} = \sqrt{\mathbf{k}_q^2 + m^2}. \quad (31)$$

This expression is further simplified by using the relation

$$\int d\mathbf{k}_p \int_{\sqrt{\mathbf{k}_p^2 + m_{\mathbf{n}_q}^2}}^{\infty} \frac{f(x) dx}{\sqrt{x^2 - \mathbf{k}_p^2 - m_{\mathbf{n}_q}^2}} = \frac{\pi^{(p+1)/2}}{\Gamma((p+1)/2)} \int_b^{\infty} dy (y^2 - m_{\mathbf{n}_q}^2)^{(p-1)/2} f(y). \quad (32)$$

The final formula can be written in a form valid for both plates and for both sides of the plate:

$$\langle j^l \rangle_j^{(1)} = -\frac{A_p}{V_q} N_D m \sum_{\mathbf{n}_q \in \mathbf{Z}^q} k_l \int_{m_{\mathbf{n}_q}}^{\infty} dx (x^2 - m_{\mathbf{n}_q}^2)^{(p-1)/2} \frac{e^{-2x|z-a_j|}}{m+x}, \quad (33)$$

with the notation

$$A_p = \frac{(4\pi)^{-(p+1)/2}}{\Gamma((p+1)/2)}. \quad (34)$$

In Eq. (33), $j = 1, 2$, $a_1 = 0$, $a_2 = a$, and $\langle j^l \rangle_j^{(1)}$ is the VEV induced by a single plate placed at $z = a_j$, so $\langle j^l \rangle_1^{(1)} = \langle j^l \rangle^{(1)}$. Note that the integral in Eq. (33) is a monotonically decreasing positive function of $m_{\mathbf{n}_q}$. An alternative expression for the plate induced part in the VEV of the fermionic current is derived in Appendix A, by using the summation formula (62).

If the length of the r -th compactified dimension, L_r , $r \neq l$, is large compared to the other length scales, the dominant contribution to the sum over n_r in Eq. (33) comes from large values of n_r . In this case, to the leading order, we can replace the corresponding series by an integral, using the relation

$$\sum_{n_r=-\infty}^{+\infty} f(2\pi|n_r + \tilde{\alpha}_r|/L_r) \rightarrow \frac{L_r}{\pi} \int_0^{\infty} dy f(y). \quad (35)$$

The double integral is reduced to the single one with the help of the formula

$$\int_0^{\infty} dy \int_{\sqrt{y^2 + b^2}}^{\infty} dx (x^2 - y^2 - b^2)^{(p-1)/2} f(x) = \frac{\sqrt{\pi} \Gamma((1+p)/2)}{2\Gamma(1+p/2)} \int_b^{\infty} du (u^2 - b^2)^{p/2} f(u), \quad (36)$$

and from Eq. (33) the corresponding expression is obtained for the topology $R^{p+2} \times (S^1)^{q-1}$. Note that this way of calculating does not work for the case $r = l$, as the leading term obtained by the replacement (35) vanishes. The asymptotic expression for large values of L_l will be given below, by using the alternative representation of the boundary induced part in the VEV given in Appendix.

In the opposite limit, i.e. when L_r is small, the behavior of the current density depends crucially whether the parameter $\tilde{\alpha}_r$ is zero or not. For $\tilde{\alpha}_r = 0$ the dominant contribution in Eq. (33) comes from the mode with $n_r = 0$, and to the leading order one has

$$\langle j^l \rangle_j^{(1)} \approx N_D (N_{D-1} L_r)^{-1} \langle j^l \rangle_{j, R^{p+1} \times (S^1)^{q-1}}^{(1)}, \quad (37)$$

where $\langle j^l \rangle_j^{(1)}$ is the corresponding quantity in $(D-1)$ -dimensional space with topology $R^{p+1} \times (S^1)^{q-1}$ and with the lengths of the compact dimensions $L_{p+2}, \dots, L_{r-1}, L_{r+1}, \dots, L_D$. For $\tilde{\alpha}_r \neq 0$, the dominant contribution comes from the region near the lower limit of the integration in Eq. (33) and we get:

$$\langle j^l \rangle_j^{(1)} \approx -\frac{N_D m}{V_q} \frac{|z - a_j|^{-(p+1)/2}}{2(4\pi)^{(p+1)/2}} \sum_{\mathbf{n}_q \in \mathbf{Z}^q} k_l m_{\mathbf{n}_q}^{(p-3)/2} e^{-2|z - a_j| m_{\mathbf{n}_q}}. \quad (38)$$

As before, the contribution of the term with $n_r = 0$ dominates and the VEV is exponentially suppressed by the factor $e^{-4\pi\tilde{\alpha}_r|z - a_j|/L_r}$. Note that this asymptotic form is valid for $r = l$ as well.

For the investigation of the boundary induced part near the plate and for large values of L_l , it is more convenient to use Eq. (65). From this expression it is seen that the boundary induced part is finite on the plate and the corresponding value is obtained by the direct substitution $z = 0$. This contrasts with the case of the fermionic condensate and the VEV of the energy-momentum tensor (see Ref. [9]) which are divergent on the boundary.

In the limit of large values of L_l the dominant contribution in Eq. (65) comes from the region near the lower limit of the integral over x . Assuming $|\tilde{\alpha}_l| < 1/2$, we can see that the contribution of the term with $n_i = 0$, $i = p+2, \dots, l-1, l+1, \dots, D$, dominates in the sum over \mathbf{n}_{q-1} . To the leading order we get

$$\langle j^l \rangle_j^{(1)} \approx -\frac{N_D L_l}{V_q} \frac{\sin(2\pi\tilde{\alpha}_l)}{(2\pi L_l)^{p/2+1}} m_l^{p/2+1} e^{-m_l L_l}, \quad (39)$$

with the notation

$$m_l^2 = \sum_{i=p+2, i \neq l}^D (2\pi\tilde{\alpha}_i/L_i)^2 + m^2. \quad (40)$$

Hence, for large values of the length of the compact dimension we have an exponential suppression. In this limit the total VEV is dominated by the boundary-free part $\langle j^l \rangle^{(0)}$. As we see, in both limits of small and large values of L_l the boundary induced part in the VEV of the fermionic current goes to zero.

In the numerical examples below we consider the simplest Kaluza-Klein model with a single compact dimension with $p = D - 2$, $q = 1$, and $k_{\mathbf{n}_q} = 2\pi|n_D + \alpha_D|/L_D$. In the left panel of Fig. 1, the current density induced by a single plate at $z = 0$ is plotted versus the parameter $\tilde{\alpha}_D$, for a fixed value $mz = 0.5$. The numbers near the curves are the corresponding values of mL_D (the length of the compact space in units of the Compton wavelength of the fermionic particle). As we already mentioned before, the current density is a periodic function of the parameter $\tilde{\alpha}_D$ with the period equal to 1. As it is seen from the graphs, the absolute value of the parameter $\tilde{\alpha}_D$, for which the current is maximum, increases with increasing the length of the compact dimension. The value of the current at the maximum decreases with increasing the length. The right panel of Fig. 1 presents the dependence of the fermionic current on the length of the compact dimension for separate values of the parameter $\tilde{\alpha}_D$ (numbers near the curves) and for $mz = 0.5$. As we already mentioned, the boundary induced part vanishes in both limits of small and large values of the compact dimension length.

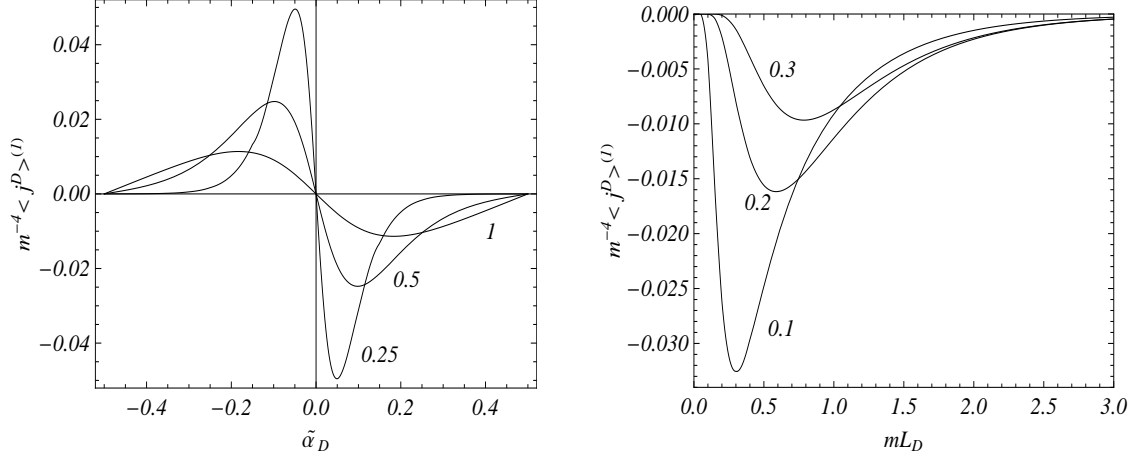


Figure 1: VEV of the current density induced by a single plate in the Kaluza-Klein model with spatial topology $R^3 \times S^1$, as a function of the parameter $\tilde{\alpha}_D$ (left plot) and of the parameter mL_D (right plot), for a fixed distance from the plate corresponding to $mz = 0.5$. The numbers near the curves are the values of mL_D (left plot) and $\tilde{\alpha}_D$ (right plot).

3.2.2 Geometry of two plates

By using Eq. (32), the total VEV in the region between two plates is presented in the form

$$\begin{aligned} \langle j^l \rangle &= \langle j^l \rangle^{(0)} + \langle j^l \rangle^{(1)} - N_D \frac{A_p}{V_q} \sum_{\mathbf{n}_q \in \mathbf{Z}^q} k_l \int_{m_{\mathbf{n}_q}}^{\infty} dx \\ &\times \frac{(x^2 - m_{\mathbf{n}_q}^2)^{(p-1)/2}}{\frac{x+m}{x-m} e^{2ax} + 1} \left[2 - m \left(\frac{e^{2zx}}{m-x} + \frac{e^{-2zx}}{m+x} \right) \right], \end{aligned} \quad (41)$$

where $m_{\mathbf{n}_q}$ is defined by Eq. (31). Combining with Eq. (33) for the geometry of a single plate, we find

$$\begin{aligned} \langle j^l \rangle &= \langle j^l \rangle^{(0)} - 2N_D \frac{A_p}{V_q} \sum_{\mathbf{n}_q \in \mathbf{Z}^q} k_l \int_{m_{\mathbf{n}_q}}^{\infty} dx \\ &\times \frac{(x^2 - m_{\mathbf{n}_q}^2)^{(p-1)/2}}{\frac{x+m}{x-m} e^{2ax} + 1} \left\{ 1 + \frac{me^{ax}}{x-m} \cosh[(a-2z)x] \right\}. \end{aligned} \quad (42)$$

As we could expect, this expression is symmetric with respect to the plane $z = a/2$. The integral in Eq. (42) is a monotonically decreasing positive function of $m_{\mathbf{n}_q}$.

The formula (42) is further simplified for a massless field:

$$\langle j^l \rangle = \langle j^l \rangle^{(0)} - 2N_D \frac{A_p}{V_q} \sum_{\mathbf{n}_q \in \mathbf{Z}^q} k_l \int_{k_{\mathbf{n}_q}}^{\infty} dx \frac{(x^2 - k_{\mathbf{n}_q}^2)^{(p-1)/2}}{e^{2ax} + 1}, \quad (43)$$

where

$$k_{\mathbf{n}_q}^2 = \sum_{i=p+2}^D [2\pi(n_i + \tilde{\alpha}_i)/L_i]^2. \quad (44)$$

Note that in this case the distribution of the fermionic current in the region between the plates is uniform. An alternative expression is obtained by making use of the expansion $(e^y + 1)^{-1} =$

$-\sum_{n=1}^{\infty}(-1)^n e^{-ny}$. Then the integral is expressed in terms of the Macdonald function and one gets

$$\langle j^l \rangle = \langle j^l \rangle^{(0)} + \frac{4N_D a^{-p/2}}{(4\pi)^{p/2+1} V_q} \sum_{\mathbf{n}_q \in \mathbf{Z}^q} k_l k_{\mathbf{n}_q}^{p/2} \sum_{n=1}^{\infty} \frac{(-1)^n}{n^{p/2}} K_{p/2}(2nak_{\mathbf{n}_q}). \quad (45)$$

At large separations between the plates, compared with the lengths of the compact directions, the dominant contribution to Eq. (45) comes from the terms with $n_i = 0$ for $|\tilde{\alpha}_i| < 1/2$ and from the terms $n_i = 0, \pm 1$ for $\tilde{\alpha}_i = \mp 1/2$. For $|\tilde{\alpha}_l| \leq 1/2$, to the leading order one finds:

$$\langle j^l \rangle \approx \langle j^l \rangle^{(0)} - \frac{2^{N_{1/2}} N_D \tilde{\alpha}_l \beta_0^{(p-1)/2}}{(2a)^{(p+1)/2} V_q L_l} e^{-4\pi a \beta_0}, \quad (46)$$

where $\beta_0^2 = \sum_{i=p+2}^D (\tilde{\alpha}_i/L_i)^2$ and $N_{1/2}$ is the number of compact dimensions for which $\tilde{\alpha}_i = \pm 1/2$, $i \neq l$. As it is seen, in this limit the boundary induced part in the VEV is exponentially small.

Extracting the parts corresponding to the single plates, the fermionic current can also be presented in the form

$$\langle j^l \rangle = \langle j^l \rangle^{(0)} + \sum_{j=1,2} \langle j^l \rangle_j^{(1)} + \Delta \langle j^l \rangle, \quad (47)$$

where the interference term is given by the expression

$$\begin{aligned} \Delta \langle j^l \rangle &= -\frac{A_p N_D}{V_q} \sum_{\mathbf{n}_q \in \mathbf{Z}^q} k_l \int_{m_{\mathbf{n}_q}}^{\infty} dx \frac{(x^2 - m_{\mathbf{n}_q}^2)^{(p-1)/2}}{\frac{x+m}{x-m} e^{2ax} + 1} \\ &\times \left[2 - \frac{m}{x+m} \left(e^{-2zx} + e^{2x(z-a)} \right) \right]. \end{aligned} \quad (48)$$

For a massless field the interference part coincides with the boundary induced part. In the limit of large separation between the plates, the dominant contribution comes from the region near the lower limit of the integration in Eq. (48). To the leading order we get

$$\begin{aligned} \Delta \langle j^l \rangle &\approx -\frac{2^{N_{1/2}} \pi N_D \tilde{\alpha}_l m_0^{(p-1)/2}}{V_q (4\pi a)^{(p+1)/2} L_l} \frac{m_0 - m}{m_0 + m} e^{-2am_0} \\ &\times \left[2 - \frac{m}{m_0 + m} \left(e^{-2zm_0} + e^{2m_0(z-a)} \right) \right], \end{aligned} \quad (49)$$

where

$$m_0^2 = \sum_{i=p+2}^D (2\pi \tilde{\alpha}_i/L_i)^2 + m^2. \quad (50)$$

For a massless field this result is reduced to Eq. (46). Hence, in the limit under consideration, the interference effects between the boundaries are exponentially suppressed.

Up to now, we have considered the region between the plates, $0 < z < a$. For the regions $z < 0$ and $z > a$, the VEV of the components of the fermionic current along the compact dimension z_l is given by the expressions:

$$\begin{aligned} \langle j^l \rangle &= \langle j^l \rangle^{(0)} + \langle j^l \rangle_1^{(1)}, \quad z < 0, \\ \langle j^l \rangle &= \langle j^l \rangle^{(0)} + \langle j^l \rangle_2^{(1)}, \quad z > a, \end{aligned} \quad (51)$$

with the plate induced part given by Eq. (33). In particular, the boundary induced part vanishes in these regions, for a massless field.

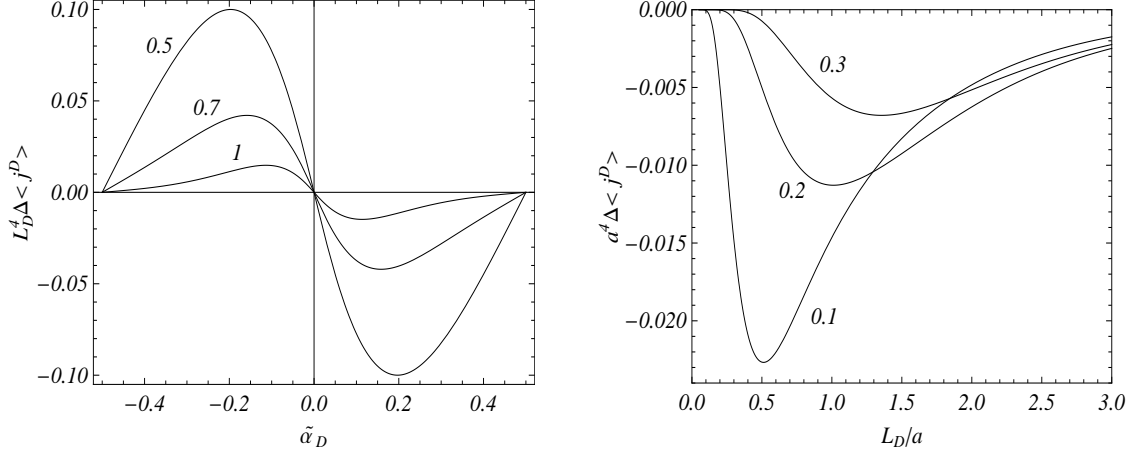


Figure 2: Boundary induced part of the fermionic current versus $\tilde{\alpha}_D$ (left plot) and L_D/a (right plot) in the region between two plates for the model with spatial topology $R^3 \times S^1$ and for a massless field. The numbers near the curves are the values of a/L_D (left plot) and of $\tilde{\alpha}_D$ (right plot).

As in the case of a single plate, in the numerical example we consider the model with spatial topology $R^3 \times S^1$ and with the length of the compact dimension L_D . In Fig. 2, the boundary induced part in the VEV of the corresponding fermionic current is plotted for a massless field in the region between two plates, as a function of the parameter $\tilde{\alpha}_D$ (left plot) and as a function of L_D/a (right plot). The numbers near the curves correspond to the values of the ratio a/L_D for the left plot and to the values of $\tilde{\alpha}_D$ for the right plot. Similar to the single plate case, the boundary induced part vanishes in both limits of small and large values of the compact dimension length.

3.3 Fermionic current in conformally-flat spacetimes

From quantum field theory in curved spacetime it is well-known (see, for instance, Ref. [16]) that, in conformally-flat spacetimes, the expectation values of bilinear field combinations for conformally invariant fields are related to the corresponding quantities in flat spacetime by a conformal transformation. By taking into account that a massless fermionic field is conformally invariant in all spatial dimensions, we can use the results given above for the generation of the topological and boundary induced parts in the VEV of the fermionic current for conformally-flat spacetimes with spatial topology $R^{p+1} \times (S^1)^q$ and with the line-element

$$ds^2 = \Omega^2(z_l)[dt^2 - \sum_{i=1}^D (dz_i)^2], \quad (52)$$

where, as before, $0 \leq z_l \leq L_l$, $l = p+2, \dots, D$. The functions $\Omega(z_l)$ are assumed to be periodic along the compact dimensions. The Dirac matrices in this spacetime, $\gamma_{(\Omega)}^\mu$, are related to the matrices in flat spacetime by $\gamma_{(\Omega)}^\mu = e_l^\mu \gamma^l$, where $e_l^\mu = \Omega^{-1} \delta_l^\mu$ is the corresponding tetrad field. If $\psi_{(\Omega)}$ is a massless fermion field in the spacetime with the line-element (52), then we have the following conformal transformation: $\psi_{(\Omega)} = \Omega^{-D/2} \psi$, $\bar{\psi}_{(\Omega)} = \Omega^{-D/2} \bar{\psi}$. By taking into account that, for the normal to the boundaries, one has $n_{(\Omega)\mu} = \Omega n_\mu$, we see that the bag boundary condition $[1 + i\gamma_{(\Omega)}^\mu n_{(\Omega)\mu}] \psi_{(\Omega)} = 0$ is invariant under the conformal transformation. Assuming

the presence of two boundaries at $z = 0$ and $z = a$ ($z_{p+1} \equiv z$), with bag boundary conditions, for the fermionic current in the spacetime (52), we get

$$\langle j^\mu \rangle_{(\Omega)} = \langle j^\mu \rangle_{(\Omega), R^D} + \Omega^{-D-1} \langle j^\mu \rangle. \quad (53)$$

Here, the first term in the right-hand side is the corresponding VEV for a spacetime with the line-element (52) and with spatial topology R^D , and the second term is induced by the nontrivial topology and by the boundaries. With this form, the renormalization is needed for the first term only. For the special cases of de Sitter and anti-de Sitter (AdS) spacetimes, one has $\Omega^2 = 1/(Ht)^2$ and $\Omega^2 = 1/(kz)^2$, respectively.

Let us consider the case of AdS bulk in detail. The boundaries in AdS spacetime can play the role of branes in higher-dimensional generalizations of Randall-Sundrum-type braneworlds with toroidally compactified internal spaces. In these models the coordinate z is compactified on an orbifold S^1/Z_2 , and the branes are on the two fixed points. The left/right boundaries correspond to the hidden/visible branes. By taking into account that $z = 0$ represents the AdS boundary ($z = \infty$ corresponds to the AdS horizon), we will assume that the boundaries are located at $z = a_1 \neq 0$ and $z = a_2$, $a_1 < a_2$. The physical coordinate in the direction perpendicular to the branes corresponds to $y = k^{-1} \ln(kz)$, with k^{-1} being the AdS radius. The physical distance between the branes, in terms of this coordinate, is given by $y_0 = k^{-1} \ln(a_2/a_1)$. To discuss the physics from the point of view of a D -dimensional observer residing on the visible brane, we introduce rescaled coordinates z'_l on this brane as $z'_l = z_l/(ka_2)$. With these coordinates the warp factor in the metric (52) is equal to one at the brane $z = a_2$, and they are physical coordinates for an observer on this brane. The corresponding lengths of the compact dimensions are given by $L'_l = L_l/(ka_2)$. For the part in the VEV of the fermionic current induced by the hidden brane and measured by an observer on the visible brane, from Eqs. (45) and (53) one finds

$$\begin{aligned} \langle j'^l \rangle_{\text{AdS}}^{(b)} &= 4N_D k^{p/2} \frac{(1 - e^{-ky_0})^{-p/2}}{(4\pi)^{p/2+1} V'_q} \sum_{\mathbf{n}_q \in \mathbf{Z}^q} k'_l k'^{p/2}_{\mathbf{n}_q} \\ &\times \sum_{n=1}^{\infty} \frac{(-1)^n}{n^{p/2}} K_{p/2}(2n(1 - e^{-ky_0})k'_{\mathbf{n}_q}/k), \end{aligned} \quad (54)$$

where the expressions for the primed quantities in the right-hand side are obtained from the corresponding expressions above by the replacement $L_l \rightarrow L'_l$. When the left brane tends to the AdS boundary, $a_1 \rightarrow 0$, the fermionic current goes to a finite limiting value.

4 Fermionic current in finite-length carbon nanotubes

In this section, we apply general formulas given above, for the investigation of the fermionic current in finite-length carbon nanotubes. Because of their unique electronic properties and potential applications in nanotechnology, carbon nanotubes have attracted enormous attention (see, for instance, Ref. [17]). A single-walled cylindrical nanotube can be thought of, as a graphene sheet rolled in a cylindrical form, with diameters ranging from 1 nm to 5 nm. Multi-walled carbon nanotubes are made of coaxial nanotube cylinders. The diameter of the outer tubes for multi-walled nanotubes can be of the order of 500 nm. The electronic coupling between separate layers in these nanotubes is weak, and the results given below can be applied for both single-walled and multi-walled carbon nanotubes. The low-energy excitations of the electronic subsystem in a graphene sheet are well described by the (2+1)-dimensional Dirac model containing a pair of spinors ψ_A and ψ_B (for a review see Ref. [3]). The latter correspond to the

two different triangular sublattices of the honeycomb lattice of graphene. Recently, a number of predictions of the Dirac model have been confirmed experimentally with a high precision. For carbon nanotubes the background space for the (2+1)-dimensional Dirac model has the topology $R^1 \times S^1$. The field equation for the separate spinors reads

$$(iv_F^{-1}\gamma^0 D_0 + i\gamma^l D_l - m)\psi_J = 0, \quad (55)$$

where $J = A, B$ and $v_F \approx 10^8$ cm/s is the Fermi velocity of electrons. The mass (gap) term in Eq. (55) can be generated by a number of mechanisms (see, for example, Ref. [18]).

The electrical properties of carbon nanotubes crucially depend on diameter and chirality. Depending on the chirality, the nanotubes are either metallic or semiconducting. The chirality also determines the periodicity condition along the compact dimension for the fields ψ_J . In metallic nanotubes, the periodic boundary condition is realized with the value $\alpha_l = 0$ for the phase in Eq. (3). For semiconducting nanotubes, depending on the chiral vector, there are two classes of inequivalent periodicity conditions, corresponding to $\alpha_l = \pm 1/3$. These phases have opposite signs for the sublattices A and B .

Although carbon nanotubes are typically longer than a micrometer, recently a number of techniques have been developed for the synthesis of ultra-short carbon nanotubes with lengths ranging between 20 and 80 nm (see, for instance, Ref. [19]). This type of nanotubes are especially useful in biomedical applications. In the long-wavelength description of the electronic subsystem, the Dirac fields ψ_J live on the cylinder surface and for finite-length nanotubes additional boundary conditions should be imposed at the edges. As the electrons are confined between two edges of the nanotube, it is natural to impose the bag boundary conditions at the edges. As we mentioned before, the latter results in zero fermion flux through the boundaries. The effect of these boundary conditions on the fermionic current can be investigated by using the expressions from the previous section. For nanotubes the corresponding values for the dimensions are as follows: $D = 2$, $p = 0$, $q = 1$. Another type of boundary induced effect, i.e. the Casimir effect between two graphene sheets or for a graphene sheet interacting with a metal, has been investigated in Refs. [20], using either the hydrodynamic model or the Dirac model for quasiparticles in graphene (for a comparison of the results obtained by these two approaches see Ref. [21]).

Before considering finite-length effects, we recall the result for the fermionic current in an infinite-length nanotube. The corresponding expression is obtained from Eq. (28) with $\alpha_l = \alpha$ and $L_2 = L$. Summing the contributions from the two sublattices and taking into account that, for them the phases α have opposite signs, for the total fermionic current we find [12]

$$\langle j^2 \rangle_{(\text{cn})}^{(0)} = \frac{2v_F}{\pi L^2} \sum_{n=1}^{\infty} \cos(2\pi n\alpha) \sin(2\pi n\Phi/\Phi_0) \frac{1 + nLm}{n^2 e^{nLm}}, \quad (56)$$

where $\alpha = 0, 1/3$ for metallic and semiconducting nanotubes, respectively. In Eq. (56), we have expressed the component of the vector potential along the compact dimension in terms of the magnetic flux Φ passing through the cross section of the nanotube: $\Phi = A_2 L$. Note that in Eq. (56) and in the formulas below, we give the fermionic current for a given spin component. The total current is obtained multiplying by the number of spin components, which is 2 for graphene. From Eq. (56) it follows that, in the absence of the magnetic flux, the total fermionic current vanishes, due to the cancellation of contributions from the two sublattices.

Next, we consider a semi-infinite nanotube which corresponds to the single plate geometry discussed in the previous section. Summing the contributions from two different sublattices,

from the general formula (33) one gets:

$$\langle j^2 \rangle_{(\text{cn})}^{(1)} = -\frac{mv_F}{\pi L} \sum_{j=+,-} \sum_{n=-\infty}^{+\infty} k_n^{(j)} \int_{m_n^{(j)}}^{\infty} dx \frac{e^{-2xz}}{\sqrt{x^2 - m_n^{(j)2}}} \frac{1}{m+x}, \quad (57)$$

with the notation

$$m_n^{(\pm)} = \sqrt{k_n^{(\pm)2} + m^2}, \quad k_n^{(\pm)} = 2\pi(n + \Phi/\Phi_0 \pm \alpha)/L. \quad (58)$$

In Eq. (57), $z = 0$ corresponds to the edge of the nanotube. An alternative expression is obtained by using Eq. (65):

$$\begin{aligned} \langle j^2 \rangle_{(\text{cn})}^{(1)} &= -\frac{mv_F}{\pi^2} \sum_{j=+,-} \sin(2\pi(\Phi/\Phi_0 + j\alpha)) \int_0^{\infty} dx x \\ &\quad \times [\cosh(L\sqrt{x^2 + m}) - \cos(2\pi(\Phi/\Phi_0 + j\alpha))]^{-1} \\ &\quad \times \int_0^1 dy \frac{m \cos(2zxy) - xy \sin(2zxy)}{(m^2 + x^2 y^2) \sqrt{1 - y^2}}. \end{aligned} \quad (59)$$

This expression is more convenient for the evaluation of the current near the edge and for large values of the nanotube diameter. The asymptotic expressions in various limiting cases are directly obtained from those for general D discussed in the previous section. The electric current corresponding to the VEV of the fermionic current discussed in this section is of the order $|e|v_F/L$. The persistent currents in normal metal rings with this order of magnitude have been recently detected in Ref. [22].

In Fig. 3 we display the dependence of $L^2 \langle j^2 \rangle_{(\text{cn})}^{(1)}$ on the magnetic flux, in units of the flux quantum, for $mz = 0.5$. The numbers near the curves correspond to the values of mL . The left/right panel correspond to metallic/semiconducting nanotubes.

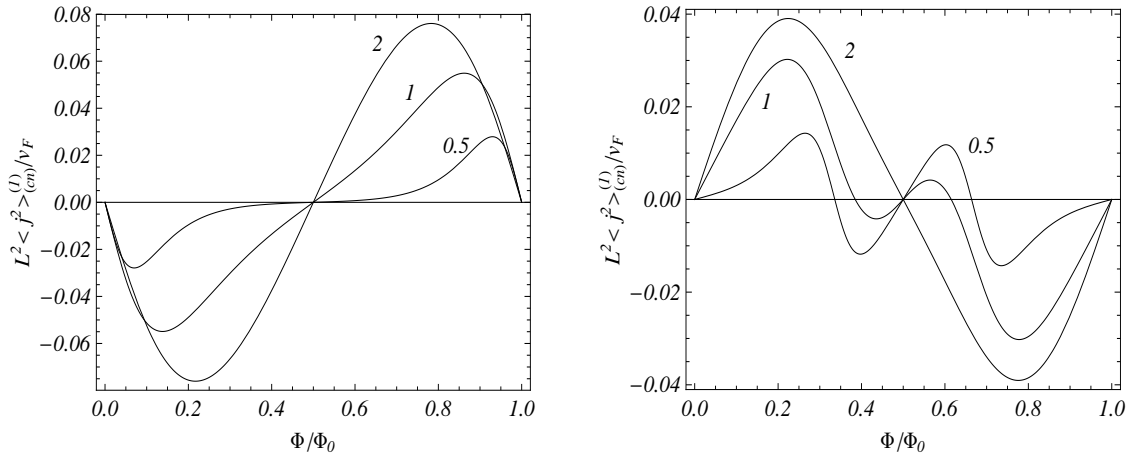


Figure 3: Edge induced part in the fermionic current for semi-infinite metallic (left panel) and semiconducting (right panel) carbon nanotubes as a function of the magnetic flux. The graphs are plotted for $mz = 0.5$ and for different values of the parameter mL (numbers near the curves).

In the case of a nanotube of finite length, a , the general expression (42) takes the form

$$\begin{aligned} \langle j^2 \rangle_{(\text{cn})} &= \langle j^2 \rangle_{(\text{cn})}^{(0)} - \frac{2v_F}{\pi L} \sum_{n=-\infty}^{+\infty} \sum_{j=+,-} k_n^{(j)} \\ &\times \int_{m_n^{(j)}}^{\infty} dx \frac{1 + \frac{m}{x-m} e^{ax} \cosh[(a-2z)x]}{\left(\frac{x+m}{x-m} e^{2ax} + 1\right) \sqrt{x^2 - m_n^{(j)2}}}. \end{aligned} \quad (60)$$

In the absence of a magnetic flux, the sublattices give opposite contributions to the fermionic current, and the latter vanishes. For a massless field one finds

$$\langle j^2 \rangle_{(\text{cn})} = \langle j^2 \rangle_{(\text{cn})}^{(0)} + \frac{2v_F}{\pi L} \sum_{n=-\infty}^{+\infty} \sum_{j=+,-} k_n^{(j)} \sum_{s=1}^{\infty} (-1)^s K_0(2sa|k_n^{(j)}|). \quad (61)$$

As already mentioned, the fermionic current is a periodic function of the magnetic flux, with period equal to the flux quantum Φ_0 .

In Fig. 4 we have plotted the boundary induced part, $\langle j^2 \rangle_{(\text{cn})}^{(\text{b})} = \langle j^2 \rangle_{(\text{cn})} - \langle j^2 \rangle_{(\text{cn})}^{(0)}$, for a massless field in metallic (left panel) and semiconducting (right panel) finite-length nanotubes, as a function of the magnetic flux. Numbers near the curves correspond to the values of the parameter a/L .

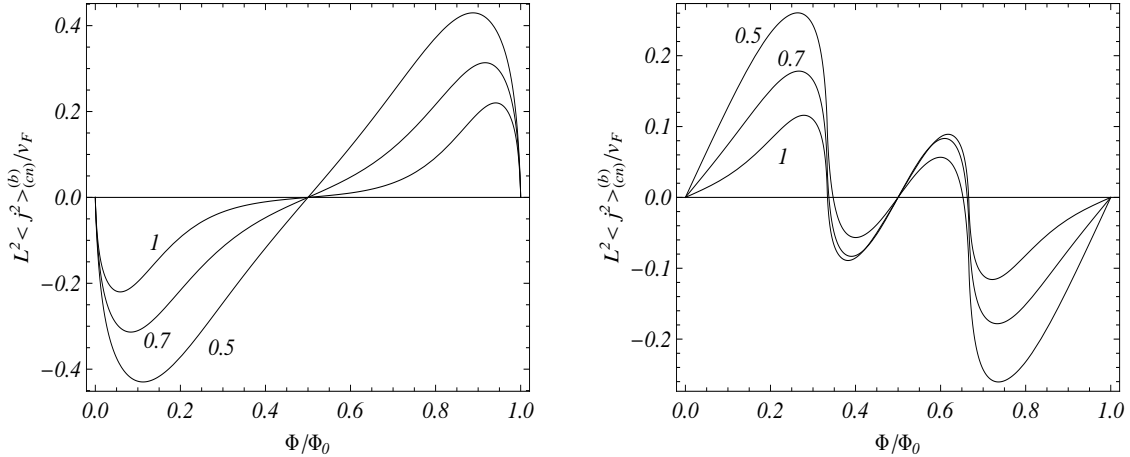


Figure 4: Boundary induced part in the VEV of the fermionic current for a massless field in finite-length metallic (left plot) and semiconducting (right plot) nanotubes, as a function of the magnetic flux. Numbers near the curves correspond to the values of the parameter a/L .

The dependence of the current density on the length of the nanotube is displayed in Fig. 5, in the model with a massless fermionic field. The numbers near the curves correspond to the length of the compact dimension in units of a fixed length scale a_0 , and for the magnetic flux we have taken the value $\Phi = 0.8\Phi_0$. The left and right panels correspond to metallic and semiconducting nanotubes. As it is seen, for long nanotubes the edge induced effects are small and the current tends the corresponding value for an infinite length nanotube.

5 Conclusion

We have investigated combined effects of compact spatial dimensions and boundaries on the VEV of the fermionic current. The geometry of boundaries is given by two parallel plates on

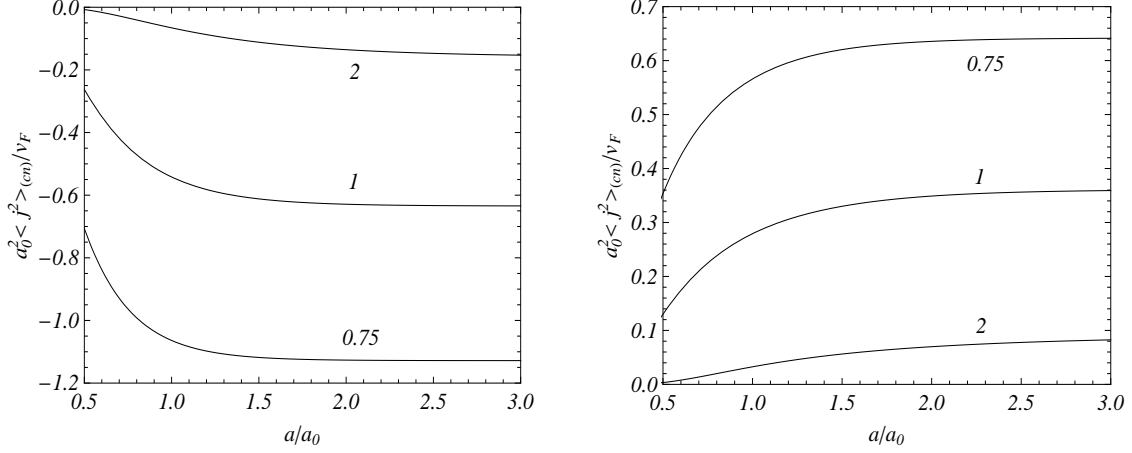


Figure 5: VEV of the fermionic current for a massless field in metallic (left plot) and semiconducting (right plot) nanotubes, as a function of the tube length. The graphs are plotted for $\Phi = 0.8\Phi_0$ and the numbers near the curves correspond to the values of the parameter L/a_0 .

which the Dirac fermion field obeys MIT bag boundary conditions. Imposing these conditions in the region between the plates leads to the discrete eigenvalues for the component of the momentum perpendicular to the plates. For the case of a massive field, they are solutions of the transcendental equation (12). Along the compact dimensions, the periodicity conditions (3) are imposed with constant phases α_l . In addition, we assume the presence of a constant gauge field which leads to the Aharonov-Bohm-like effect on the VEV of the fermionic current. The application of the summation formula (15) allowed us to decompose the VEV as the sum of topological, single plate and interference parts. In this way the renormalization is reduced to the one for the boundary-free geometry.

Similar to the case of the geometry without boundaries, the VEV of the charge density vanishes. As for what concerns the spatial components of the current density, only the components along compact dimensions are non-vanishing. The VEV of the corresponding fermionic current depends on the phases in the periodicity conditions and on the components of the vector potential in the combination (23). The VEV is a periodic odd function of this parameter with the period equal to 1. It vanishes for special cases $\tilde{\alpha}_l = 0$ and $\tilde{\alpha}_l = 1/2$. This is the case for untwisted and twisted fermion fields in the absence of the gauge field.

Firstly, we have considered the geometry of a single plate. The boundary induced part in the VEV for the component of the fermionic current along the l -th compact dimension is given by Eq. (33). This part vanishes for a massless field. An alternative expression, Eq. (65), is derived in Appendix A, by using the summation formula (62). Unlike the case of the fermionic condensate and the VEV of the energy-momentum tensor, the VEV of the fermionic current is finite on the boundary. In both limits of small and large values of the compact dimension length, the boundary induced part vanishes. At large distances from the plate, the asymptotic behavior of the fermionic current essentially depends on the phases present in the periodicity conditions along the compact dimensions.

In the region between two plates, the VEV of the fermionic current is presented in the form (42), where the first term on the right-hand side is the corresponding VEV in the boundary-free space with topology $R^{p+1} \times (S^1)^q$. The second term is induced by the boundaries. An alternative representation is given by Eq. (47) with the interference term defined by Eq. (48). For a massless field the distribution of the boundary induced part is uniform and is presented in

two equivalent forms, Eqs. (43) and (45). At large separations between the plates the boundary induced part is exponentially small (see Eq. (49)).

In the massless case the Dirac equation is conformally invariant for all spacetime dimensions. By taking into account that the bag boundary condition also is conformally invariant, and using the expression given above, we can generate the VEV of the fermionic current in conformally-flat spacetimes with compact spatial dimensions in the presence of boundaries. The corresponding VEV is given by Eq. (53), where the first term in the right-hand side is the VEV for a conformally-flat spacetime with trivial topology, in the absence of boundaries, and the second term is induced by the nontrivial topology and by the boundaries. Important special cases correspond to background de Sitter and anti-de Sitter spacetimes. As an example, we have considered the fermionic current induced on the visible brane in higher-dimensional generalizations of Randall-Sundrum-type braneworlds with internal spaces.

As an application of the general formulas, in Sect. 4, we have considered the VEV of the fermionic current in finite-length carbon nanotubes, described within the framework of the Dirac-like theory for the electronic subsystem. Recently a number of techniques allowed one to synthesize ultra-short carbon nanotubes which are especially useful in medical applications. For this type of nanotubes, the tube length can be of the order of magnitude of the compact dimension length (this is especially the case for the outermost tubes of multi-walled nanotubes) and the finite length effects may be important. The corresponding expressions for the VEV of the fermionic current are obtained by summing the contributions of the two triangular sublattices of the graphene lattice, with opposite signs of the phases along the compact dimension. Due to the cancellation between these sublattices, the current vanishes in the absence of a magnetic flux through the cross section of the nanotube. A magnetic flux through the cross section of the nanotube will break the symmetry allowing the current to flow along the compact dimension. The current is a periodic function of the flux with the period of the flux quantum Φ_0 . The pure topological contribution is then given by Eq. (56), where the values $\alpha = 0$ and $\alpha = 1/3$ correspond to metallic and to semiconducting nanotubes, respectively. For a semi-infinite nanotube, the part induced by the edge is presented in two equivalent forms, Eqs. (57) and (59). For a finite-length nanotube the VEV of the current is given by Eqs. (60) and (61) for massive and massless fields, respectively. For long nanotubes the interference effects between the edges are small and the single edge parts dominate.

Acknowledgments

A.A.S. gratefully acknowledges the hospitality of the INFN, Laboratori Nazionali di Frascati (Frascati, Italy) where part of this work was done.

A Alternative representation for a single plate induced part

An alternative representation for the part in the VEV of the fermionic current, induced by a single plate at $z = 0$, can be obtained by applying to the series over n_l in Eq. (27) the summation formula [8, 23]

$$\begin{aligned} \sum_{n_l=-\infty}^{\infty} g(n_l + \tilde{\alpha}_l) f(|n_l + \tilde{\alpha}_l|) &= \int_0^{\infty} du [g(u) + g(-u)] f(u) \\ &+ i \int_0^{\infty} du [f(iu) - f(-iu)] \sum_{\lambda=\pm 1} \frac{g(i\lambda u)}{e^{2\pi(u+i\lambda\tilde{\alpha}_l)} - 1}. \end{aligned} \quad (62)$$

For the corresponding series in Eq. (27) one has $g(u) = u$ and the first integral in the right-hand side of this formula vanishes. By integrating over \mathbf{k}_p with the help of the analog of Eq. (32), the VEV is presented in the form

$$\begin{aligned} \langle j^l \rangle^{(1)} &= -\frac{N_D A_p}{2\pi V_q} m L_l \sin(2\pi \tilde{\alpha}_l) \sum_{\mathbf{n}_{q-1} \in \mathbf{Z}^{q-1}} \int_0^\infty dx \left(\frac{e^{2ixz}}{m - ix} + \frac{e^{-2ixz}}{m + ix} \right) \\ &\times \int_0^\infty \frac{dy y}{\sqrt{x^2 + m_{\mathbf{n}_{q-1}}^2}} \frac{(y^2 - x^2 - m_{\mathbf{n}_{q-1}}^2)^{(p-1)/2}}{\cosh(y L_l) - \cos(2\pi \tilde{\alpha}_l)}, \end{aligned} \quad (63)$$

with the notation

$$m_{\mathbf{n}_{q-1}}^2 = \sum_{i=p+2, i \neq l}^D [2\pi(n_i + \tilde{\alpha}_i)/L_i]^2 + m^2. \quad (64)$$

Next, introducing instead of y a new integration variable $t = \sqrt{y^2 - x^2 - m_{\mathbf{n}_{q-1}}^2}$, we pass to polar coordinates in the plane (x, t) . After some additional transformations, the expression for the VEV of the fermionic current reads

$$\begin{aligned} \langle j^l \rangle^{(1)} &= -\frac{N_D A_p}{\pi V_q} m L_l \sin(2\pi \tilde{\alpha}_l) \sum_{\mathbf{n}_{q-1} \in \mathbf{Z}^{q-1}} \int_0^\infty dx x^{p+1} \\ &\times [\cosh(L_l \sqrt{x^2 + m_{\mathbf{n}_{q-1}}^2}) - \cos(2\pi \tilde{\alpha}_l)]^{-1} \\ &\times \int_0^1 dy \frac{m \cos(2zxy) - xy \sin(2zxy)}{(m^2 + x^2 y^2)(1 - y^2)^{(1-p)/2}}. \end{aligned} \quad (65)$$

Note that in a model with a single compact dimension one has $m_{\mathbf{n}_{q-1}} = m$ and the summation in Eq. (65) is absent. By numerical calculations we have checked the equivalence of Eqs. (33) and (65).

References

- [1] E. Elizalde, S.D. Odintsov, A. Romeo, A.A. Bytsenko and S. Zerbini, *Zeta Regularization Techniques with Applications* (World Scientific, Singapore, 1994); V.M. Mostepanenko and N.N. Trunov, *The Casimir Effect and Its Applications* (Clarendon, Oxford, 1997); K.A. Milton, *The Casimir Effect: Physical Manifestation of Zero-Point Energy* (World Scientific, Singapore, 2002); M. Bordag, G.L. Klimchitskaya, U. Mohideen, and V.M. Mostepanenko, *Advances in the Casimir Effect* (Oxford University Press, Oxford, 2009); *Lecture Notes in Physics: Casimir Physics*, Vol. 834, edited by D. Dalvit, P. Milonni, D. Roberts, and F. da Rosa (Springer, Berlin, 2011).
- [2] A. Linde, JCAP **0410**, 004 (2004).
- [3] A.H. Castro Neto, F. Guinea, N.M.R. Peres, K.S. Novoselov, and A.K. Geim, Rev. Mod. Phys. **81**, 109 (2009).
- [4] E. Elizalde, Phys. Lett. B **516**, 143 (2001); C.L. Gardner, Phys. Lett. B **524**, 21 (2002); K.A. Milton, Grav. Cosmol. **9**, 66 (2003); E. Elizalde, J. Phys. A **39**, 6299 (2006); B. Green and J. Levin, JHEP **0711**, 096 (2007); P. Burikham, A. Chatrabhuti, P. Patcharamaneepakorn, and K. Pimsamarn, JHEP **0807**, 013 (2008).

- [5] G.L. Klimchitskaya, U. Mohidden, and V.M. Mostepanenko, *Rev. Mod. Phys.* **81**, 1827 (2009).
- [6] H.B. Cheng, *Phys. Lett. B* **643**, 311 (2006); H.B. Cheng, *Phys. Lett. B* **668**, 72 (2008); S.A. Fulling and K. Kirsten, *Phys. Lett. B* **671**, 179 (2009); K. Kirsten and S.A. Fulling, *Phys. Rev. D* **79**, 065019 (2009); E. Elizalde, S.D. Odintsov, and A.A. Saharian, *Phys. Rev. D* **79**, 065023 (2009); L.P. Teo, *Phys. Lett. B* **672**, 190 (2009); L.P. Teo, *Nucl. Phys. B* **819**, 431 (2009); L.P. Teo, *JHEP* **0906**, 076 (2009); L.P. Teo, *JHEP* **0911**, 095 (2009).
- [7] K. Poppenhaeger, S. Hossenfelder, S. Hofmann, and M. Bleicher, *Phys. Lett. B* **582**, 1 (2004); A. Edery and V.N. Marachevsky, *Phys. Rev. D* **78**, 025021 (2008); A. Edery and V.N. Marachevsky, *JHEP* **0812**, 035 (2008); F. Pascoal, L.F.A. Oliveira, F.S.S. Rosa, and C. Farina, *Braz. J. Phys.* **38**, 581 (2008); L. Perivolaropoulos, *Phys. Rev. D* **77**, 107301 (2008).
- [8] S. Bellucci and A.A. Saharian, *Phys. Rev. D* **79**, 085019 (2009); S. Bellucci and A.A. Saharian, *Phys. Rev. D* **80**, 105003 (2009).
- [9] E. Elizalde, S.D. Odintsov, and A.A. Saharian, *Phys. Rev. D* **83**, 105023 (2011).
- [10] A. Flachi, J. Garriga, O. Pujolàs, and T. Tanaka, *J. High Energy Phys.* **0308**, 053 (2003); A. Flachi and O. Pujolàs, *Phys. Rev. D* **68**, 025023 (2003); A.A. Saharian, *Phys. Rev. D* **73**, 044012 (2006); A.A. Saharian, *Phys. Rev. D* **73**, 064019 (2006); A.A. Saharian, *Phys. Rev. D* **74**, 124009 (2006); R. Linares, H.A. Morales-Técolt, and O. Pedraza, *Phys. Rev. D* **77**, 066012 (2008); M. Frank, N. Saad, and I. Turan, *Phys. Rev. D* **78**, 055014 (2008).
- [11] S. Nojiri, S.D. Odintsov, and S. Zerbini, *Classical Quantum Gravity* **17**, 4855 (2000); W. Goldberger and I. Rothstein, *Phys. Lett. B* **491**, 339 (2000); A. Flachi and D. J. Toms, *Nucl. Phys. B* **610**, 144 (2001); J. Garriga, O. Pujolàs, and T. Tanaka, *Nucl. Phys. B* **605**, 192 (2001); E. Elizalde, S. Nojiri, S.D. Odintsov, and S. Ogushi, *Phys. Rev. D* **67**, 063515 (2003); A.A. Saharian and M.R. Setare, *Phys. Lett. B* **584**, 306 (2004); A. Knapman and D. J. Toms, *Phys. Rev. D* **69**, 044023 (2004); A. Flachi, A. Knapman, W. Naylor, and M. Sasaki, *Phys. Rev. D* **70**, 124011 (2004); A. A. Saharian, *Nucl. Phys. B* **712**, 196 (2005); M. Frank, I. Turan, and L. Ziegler, *Phys. Rev. D* **76**, 015008 (2007); L.P. Teo, *Phys. Lett. B* **682**, 259 (2009); A. Flachi and T. Tanaka, *Phys. Rev. D* **80**, 124022 (2009); L.P. Teo, *Phys. Rev. D* **82**, 027902 (2010); L.P. Teo, *JHEP* **1010**, 019 (2010).
- [12] S. Bellucci, A.A. Saharian, and V.M. Bardeghyan, *Phys. Rev. D* **82**, 065011 (2010).
- [13] E.R. Bezerra de Mello, V.B. Bezerra, A.A. Saharian, and V.M. Bardeghyan, *Phys. Rev. D* **82**, 085033 (2010).
- [14] A. Romeo and A. A. Saharian, *J. Phys. A: Math. Gen.* **35**, 1297 (2002).
- [15] A. A. Saharian, *The Generalized Abel-Plana Formula with Applications to Bessel Functions and Casimir Effect* (Yerevan State University Publishing House, Yerevan, 2008); Preprint ICTP/2007/082; arXiv:0708.1187.
- [16] N.D. Birrell and P.C.W. Davis, *Quantum Fields in Curved Space* (Cambridge University Press, Cambridge, England, 1982).
- [17] R. Saito, G. Dresselhaus, and M. S. Dresselhaus, *Physical Properties of Carbon Nanotubes* (Imperial College Press, London, 1998); S. Bellucci, *Phys. Stat. Sol. (c)* **2**, 34 (2005); S.

- Bellucci, Nucl. Instr. and Meth. B **234**, 57 (2005); C. Dupas, P. Houdy, and M. Lahmani (Editors), *Nanoscience: Nanotechnologies and Nanophysics* (Springer, Berlin, 2007); J.-C. Charlier, X. Blase, and S. Roche, Rev. Mod. Phys. **79**, 677 (2007).
- [18] V.P. Gusynin, V.A. Miransky, and I.A. Shovkovy, Phys. Rev. D **52**, 4718 (1995); C. Chamon, Phys. Rev. B **62**, 2806 (2000); C.-Y. Hou, C. Chamon, and C. Mudry, Phys. Rev. Lett. **98**, 186809 (2007); G. Giovannetti, P.A. Khomyakov, G. Brocks, P.J. Kelly, and J. van den Brink, Phys. Rev. B **76**, 073103 (2007); S.Y. Zhou et al., Nature Mater. **6**, 770 (2007); G.W. Semenoff, V. Semenoff, and F. Zhou, Phys. Rev. Lett. **101**, 087204 (2008); D. Haberer et al., Nano Lett. **10**, 3366 (2010); R. Balog et al., Nature Mater. **9**, 315 (2010).
- [19] Z. Gu et al., Nano Letters **2** (9), 1009 (2002); J.M. Ashcroft et al., Nanotechnology **17**, 5033 (2006).
- [20] M. Bordag, B. Geyer, G.L. Klimchitskaya, and V.M. Mostepanenko, Phys. Rev. B **74**, 205431 (2006); M. Bordag, I.V. Fialkovsky, D.M. Gitman, and D.V. Vassilevich, Phys. Rev. B **80**, 245406 (2009); G. Gómez-Santos, Phys. Rev. B **80**, 245424 (2009); I.V. Fialkovsky, V.N. Marachevsky, and D.V. Vassilevich, Phys. Rev. B **84**, 035446 (2011); D. Drosdoff and L.M. Woods, Phys. Rev. A **84**, 062501 (2011); B.E. Sernelius, Europhys. Lett. **95**, 57003 (2011); V. Svetovoy, Z. Muktadry, M. Elwenspoek, and H. Mizuta, arXiv:1108.3856; D. Drosdoff et al., arXiv:1204.4438.
- [21] Yu.V. Churkin, A.B. Fedortsov, G.L. Klimchitskaya, and V.A. Yurova, Phys. Rev. B **82**, 165433 (2010); M. Chaichian, G.L. Klimchitskaya, V.M. Mostepanenko, and A. Tureanu, arXiv:1207.3788.
- [22] H. Bluhm et al., Phys. Rev. Lett. **102**, 136802 (2009); A.C. Bleszynski-Jayich et al., Science **326**, 272 (2009).
- [23] E.R. Bezerra de Mello and A.A. Saharian, Phys. Rev. D **78**, 045021 (2008).